Materials Science and Engineering B 159–160 (2009) 264–268

Contents lists available at ScienceDirect

Materials Science and Engineering B

journal homepage: www.elsevier.com/locate/mseb

Interaction of metal impurities with extended defects in crystalline silicon and its implications for gettering techniques used in photovoltaics

M. Seibt*, D. Abdelbarey, V. Kveder[1], C. Rudolf, P. Saring, L. Stolze, O. Voß

IV. Physikalisches Institut der Universität Göttingen, Friedrich-Hund-Platz 1, D-37077 Göttingen, Germany

ARTICLE INFO

Article history:
Received 23 May 2008
Received in revised form
18 November 2008
Accepted 22 December 2008

Keywords:
Silicon
Metal impurities
Gettering
Photovoltaics

ABSTRACT

Multicrystalline silicon materials for photovoltaic applications inherently contain extended defects like grain boundaries, dislocations, microdefects and in some cases also second phase precipitates due to high concentrations of light elements (carbon, nitrogen or oxygen) and transition metal impurities. The latter are known to reduce the minority carrier lifetime and hence should be removed by gettering during solar cell processing. This paper discusses the influence of extended defects on the spatial distribution of copper- and nickel-related silicide precipitates for a model system containing a small angle grain boundary and in one part silicon oxide pecipitates partly associated with punched-out dislocations. Phosphorus-diffusion gettering under conditions of mostly precipitated metal impurities is discussed in terms of quantitative simulations. It is shown that two regimes can be distinguished where gettering kinetics are either limited by precipitate dissolution or phosphorus in-diffusion. Finally, binding of metal impurities to dislocations is considered and its effect on gettering kinetics is illustrated in terms of gettering simulations.

1. Introduction

Present-day crystalline silicon for photovoltaic applications usually contain a variety of defects ranging from point defects of various origin to extended defects like dislocations, grain boundaries, microdefects or second phase precipitates. The electrical performance of such materials, i.e. mainly their minority carrier lifetime, is closely related to metal impurities present in the feedstock or introduced during crystal growth and/or solar cell processing [1,2]. These impurities strongly interact with existing crystal defects to form complexes, accumulate at dislocations or grain boundaries in different forms, or even form silicide precipitates which simultaneously contain several metal impurities [3–5]. For quantitative understanding and simulation of gettering techniques these interactions have to be studied and described in terms of thermodynamic and kinetic models. In addition, the recombination properties of decorated crystal defects or multi-metal-precipitates have to be known if their effect on the material performance for photovoltaic applications is to be estimated.

This paper summarises recent progress in the understanding of metal impurity interaction with extended defects and the effect on gettering kinetics and efficiency. Special focus will be on the role of dislocations which are important if the lifetime reduction of intragrain regions is concerned. In addition, basic considerations of impurity interaction with dislocations can be transferred to grain boundaries. The following section is devoted to the spatial distribution of metal silicide precipitates resulting from the competition of different extended defects that act as heterogeneous nucleation sites. Phosphorus-diffusion gettering (PDG) kinetics for the case of precipitated metal impurities are described in Section 3 and two regimes are identified, i.e a dissolution-limited regime at low temperature and a phosphorus-diffusion-limited regime at high temperature. The issue of alternative processing schemes for PDG is also briefly discussed. Finally, Section 4 deals with binding of metal impurities to dislocations and its effect on PDG kinetics.

2. Spatial distribution of metal silicide precipitates

If considering second phase precipitates in crystalline silicon for photovoltaic applications one should distinguish those forming due to high concentrations of light elements (LE) like carbon, nitrogen and oxygen and those forming due to a supersaturation of fast diffusing transition metal (TM) impurities. The former are typically introduced during crystal growth in particular during extensive periods of ingot cooling to room temperature. During subsequent processing under typical conditions solid solutions of LE impurities will remain supersaturated and only sub-critical nuclei are partially re-dissolved [6] whereas larger precipitates will continue to grow.

* Corresponding author. Tel.: +49 551 394553; fax: +49 551 394560.
E-mail address: seibt@ph4.physik.uni-goettingen.de (M. Seibt).
URL: http://www.ph4.physik.uni-goettingen.de (M. Seibt).
[1] Permanent address: Insitute of Solid State Physics, RAS, Chernogolovka 142432, Russia.

0921-5107/$ – see front matter © 2009 Elsevier B.V. All rights reserved.
doi:10.1016/j.mseb.2008.12.044

On the contrary, precipitates of TM impurities may completely dissolve during wafer processing if the total TM concentration is below the solubility at processing temperature. As a result, TM impurities may substantially re-distribute in the material during high temperature processing and their repeated precipitation is likely to occur during final cooling to room temperature. The resulting distribution of metal silicide precipitates at room temperature will then critically depend on cooling conditions and the presence and spatial distribution of heterogeneous nucleation sites. The latter are typically dislocations, grain boundaries and also second phase precipitates of LE impurities or even other TM impurity precipitates. Dislocations are thought to be the most efficient nucleation sites for metal silicide precipitates in silicon which is related to their specific structure [7–9] but also small and large angle grain boundaries have found to be metal decorated to a large extent [10,11] as well as silicon oxide precipitates without secondary defects [12,13] and even wafer surfaces [14–17]. For given experimental (processing) conditions, the actual distribution of metal silicide precipitates after cooling is the result of competing nucleation sites of various type and density, and hence should be material-specific.

This has been demonstrated in a study of copper and nickel silicide precipitation in hydrophobically bonded wafers [4,5] and is briefly described below. Starting material for the experiments were two n-type Cz-grown silicon wafers with slightly different thermal history which were hydrophobically bonded with a small relative misorientation (for details of the bonding procedure, see [18]. The result of the bonding process is a silicon bicrystal containing a dislocation network consisting of screw and edge dislocations with distances of 12 nm and 372 nm, respectively, which can be viewed as a small angle grain boundary. One of the adjacent wafers, subsequently referred to as 'wafer B', contains small polyhedral silicon oxide precipitates (typical diameter: 50 nm) which are partly associated with punched-out dislocations as is revealed by transmission electron microscopy (TEM) shown in Fig. 1(a).

In-diffusion of copper into such samples at 1050 °C and subsequent moderately fast cooling results in a metal silicide particle distribution which provides some insights into the effect of different types of extended defects on precipitate nucleation. Fig. 1(b) is a light-beam induced current (LBIC) map of such a sample in cross-sectional geometry. The dislocation network separating the two initial wafers (arrows in Fig. 1(b)) exhibits a strong contrast indicating a high degree of decoration with copper silicide particles which is confirmed by TEM analyses. 'Wafer A' of the bonded sample contains a very low density of defects detectable by LBIC whereas a high density of strong contrast is detected in 'wafer B'. It is remarking to note that apparently no precipitate-free zone has been formed close to the grain boundary in wafer B as is frequently observed. This indicates that silicide precipitate nucleation there and at the bulk defects roughly occured at the same copper supersaturation. The low density of silicide precipitates in wafer A reflects the lower density of bulk defects there. As a consequence, copper out-diffusion to the surface of wafer A and to the precipitates forming at the dislocation network considerably reduces the copper concentration in wafer A and thus the precipitate density (see [4,5] for details). In summary, these experiments demonstrate how material properties and inhomogeneities of the defect density affect metal silicide precipitation and how the competition of different type of nucleation sites influences their spatial distribution.

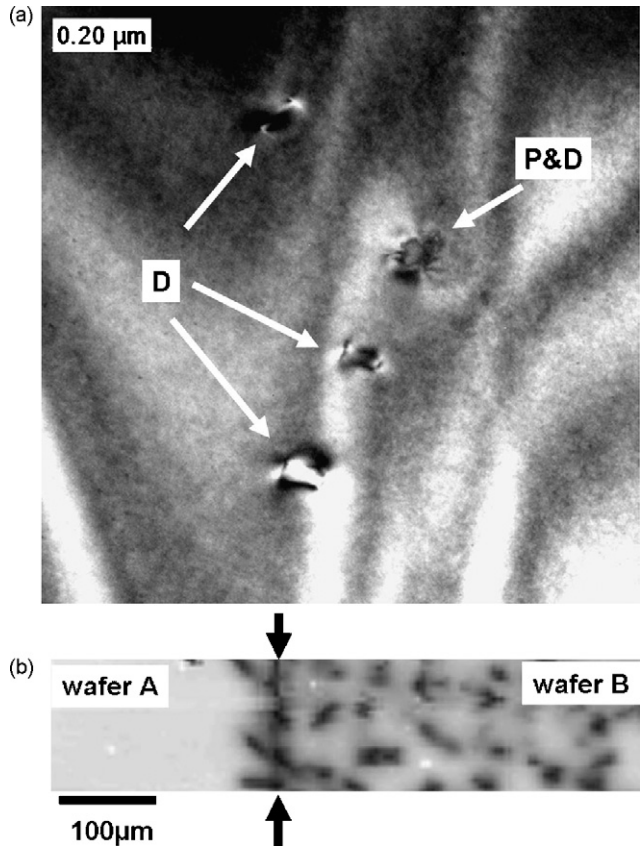

Fig. 1. Metal silicide formation at dislocation network versus bulk microdefects. (a) TEM bright-field micrograph of a silicon oxide precipitate ('P&D') with punched-out dislocation loops ('D');(b) part of a LBIC cross-section prepared from a bonded-wafer after copper in-diffusion at 1050 ° C and subsequent cooling [4,5] showing strong contrast from copper-related precipitates; the dislocation network (arrows) shows strong contrasts as well as the bulk of the right-hand side wafer which contains microdefects shown in (a).

3. PDG of precipitated metal impurities

The scenario described in the previous section resembles the situation in multicrystalline silicon wafers which contain grain boundaries and an inhomogeneous distribution of dislocations and possibly microdefects. The at least partial removal of metal impurities by phosphorus-diffusion gettering (PDG) or aluminum gettering (AlG) under such conditions faces the problem of dealing with initially precipitated impurities which, as a consequence, are immobile. Hence, dissolution of precipitates is a pre-requisite for efficient gettering which may limit gettering kinetics especially if the total metal concentration $[M]_{tot}$ exceeds the solubility $[M]_{eq}$ at gettering temperature [19] which – for solar cell processing using p-type silicon – is the temperature of the emitter formation process.

For high metal contamination levels a separate gettering step (pre-gettering) on the basis of PDG may be considered where conditions of phosphorus diffusion are optimised for gettering efficiency and a sacrificial P-doped layer for gettering is formed. In this section, we use simulations of PDG to identify and study those processes that limit gettering kinetics in the presence of metal silicide precipitates. The simulations are based on the phosphorus diffusion model by Kveder et al. [20] combined with the PDG model described in detail in [21]. Physical parameters describing thermodynamic and electronic properties of metal impurities in highly P-doped silicon have been adjusted to quantitatively describe experimental data for gold in silicon [22] and cobalt in silicon [23,24]. The simulation tool has recently been extended in order to include metal silicide precipitate dissolution and formation during cooling [19].

In this work, we use a model impurity with properties of interstitial iron in intrinsic silicon and those of cobalt in highly phosphorus doped silicon (compare [19] for details). The initial metal impurity concentration is chosen as $[M]_{ini} = 10^{14}$ cm^{-3} corresponding to the solubility of interstitial iron in intrinsic silicon at about 900 °C, which will subsequently be referred to as the solubility tempera-

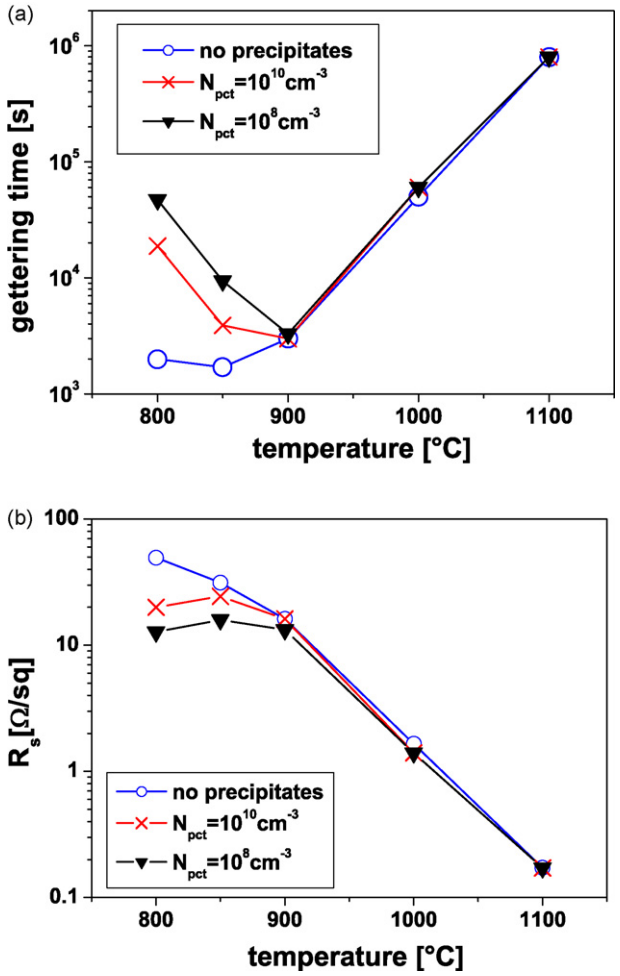

Fig. 2. Simulation of phosphorus-diffusion gettering kinetics as a function of gettering temperature for three different initial precipitate densities: (a) time needed to establish the target impurity concentration c_T starting from the initial impurity concentration c_I and (b) sheet-resistance of the highly P-doped layer when the target concentration is reached. The dissolution-limited regime ($T < 900\,^{\circ}$C) and the phosphorus-diffusion-limited regime ($T > 900\,^{\circ}$C) are clearly distinguished in both graphs.

ture, T_{eq}. PDG is performed at different temperature such that in the final state the impurity concentration is reduced to a target value of $[M]_{tar} = 10^{12}$ cm^{-3}. It should be noted that the results presented below remain valid qualitatively for other impurities and different values of $[M]_{ini}$ and $[M]_{tar}$ but will differ quantitatively.

Fig. 2 a shows the gettering time necessary to reach $[M]_{tar}$ for different gettering temperature T_G and three different initial metal impurity precipitate densities. Two regimes can easily be identified for temperatures above and below about T_{eq}, where $[M]_{ini} \simeq [M]_{eq}(T)$, which fundamentally differ by the dependence of the gettering time on the precipitate density. For $T > T_{eq}$, no influence of the precipitate density is observed which reflects the fact that all precipitates have dissolved at the very beginning of gettering; in this regime, PDG kinetics are limited by P-indiffusion, as will be discussed in Section 3.2 in more detail. For the $T < T_{eq}$ regime, gettering kinetics are slowed down by a low density of large precipitates (see Section 3.1). Part (b) of Fig. 2 shows the effect on the sheet resistance R_S of the highly P-doped region which is reached at the end of the gettering treatment. Especially those values of R_S reached in the P-diffusion-limited regime are not suitable for solar cell emitters implying that only sacrificial P-doped layers as part of a pre-gettering treatment can be formed here.

3.1. Dissolution-limited regime

In the dissolution-limited regime for $T_G < T_{eq}$ metal silicide precipitates are present almost during the entire gettering process which reduces the effective diffusion coefficient of impurity atoms due to the fact that $[M] \gg [M]_{eq}(T_G)$ during most of the gettering process. Fig. 3 shows snapshots of depth profiles for phosphorus, gettered metal impurities (mainly phosphorus–metal pairs), inter-

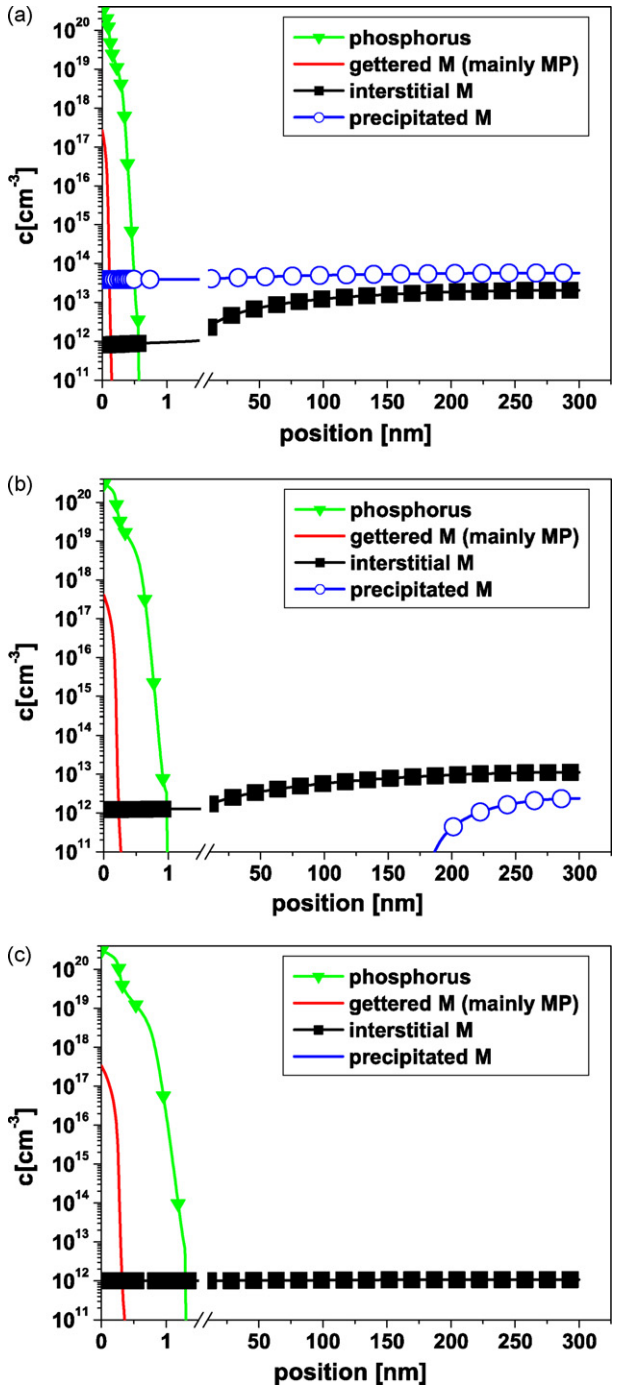

Fig. 3. Concentration profiles of P (triangles), gettered M (solid line), interstitial M (squares) and precipitated M (open circles) in the dissolution-limited regime ($T = 900\,^{\circ}$C) for different gettering times t_G: (a) small t_G: partial dissolution of precipitates gradually establishing the solubility of interstital M; (b) medium t_G: dissolution of precipitates in the front-part of the wafer; (c) large t_G: reaching of the target concentration at the end of the PDG process; partial re-precipitation of the remaining interstitial M is not included.

stitially dissolved metal atoms and those in silicide precipitates for successive gettering times. At the onset of gettering (Fig. 3(a)), silicide precipitates partly dissolve to approximately establish the solubility of the interstitial metal species at T_G. In the course of gettering, precipitates completely dissolve starting from small depths beneath the highly P-doped layer (Fig. 3(b)). Finally, precipitates have dissolved throughout the wafer and $[M]_{tar}$ is reached as depicted in Fig. 3(c). Since for a fixed total metal concentration precipitate dissolution is slowest for a low density of large precipitates, gettering kinetics will depend on the precipitate density as shown in Fig. 1.

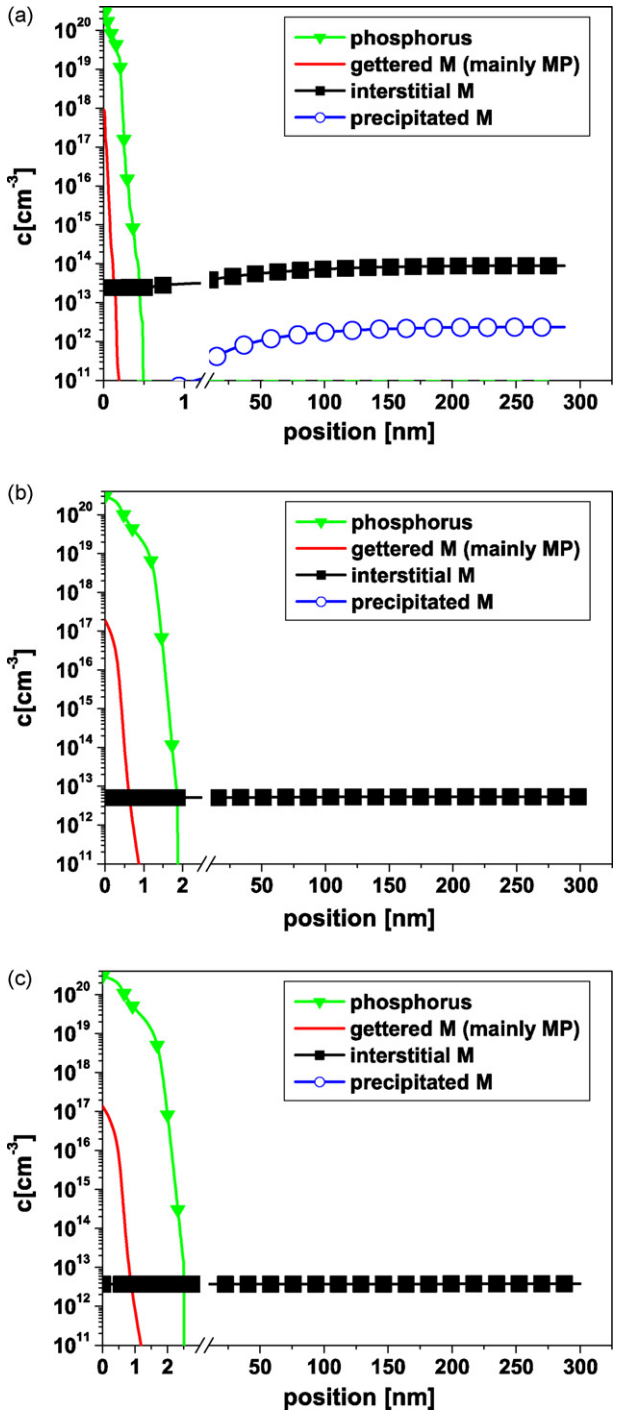

Fig. 4. Concentration profiles of P (triangles), gettered M (solid line), interstitial M (squares) and precipitated M (open circles) in the PD-limited regime ($T = 1000\,^{\circ}C$) for different gettering times t_G—(a) small t_G: partial dissolution of precipitates gradually establishing the solubility of interstital M; (b) medium t_G: complete dissolution of precipitates in the whole wafer; (c) large t_G: target concentration almost reached; once precipitates have completely dissolved, gettering kinetics are limited by phosphorus indiffusion.

3.2. Phosphorus-diffusion-limited regime

For $T_G > T_{eq}$ the situation is fundamentally different. Fig. 4 shows snapshots of depth profiles for the same species as Fig. 3 and demonstrates the difference: at the very beginning of gettering (Fig. 4(a)) metal silicide precipitates completely dissolve leading to an almost depth-independent concentration profile of the interstitial metal species (Fig. 4(b)). Here, a quasi-equilibrium between the intrinsic bulk and the highly P-doped region is established for the interstitial metal species [21]. Hence, further reduction of its (homogeneous) concentration is inevitably linked to an extension of the highly P-doped layer by phosphorus in-diffusion which consequently limits gettering kinetics (Fig. 4(c)). The increase of t_G with increasing PDG temperature then basically reflects the decreasing segregation coefficient between highly P-doped and intrinsic silicon which more than compensates for the increasing mobility of phosphorus.

3.3. Alternative processing schemes for PDG

The two regimes discussed above are of physical significance and inevitably limit PDG efficiency for isothermal processing. In addition, if several metal impurities are simultaneously present both limiting effects may be active simultaneously which complicates strategies for PDG optimisation. We have recently shown that PDG efficiency can strongly be enhanced if the condition of isothermal processing is dropped [19]. In fact, gettering schemes successively combining both regimes such that: (i) precipitate dissolution and phosphorus drive-in is facilitated during an initial (short) high temperature step ($T > T_{eq}$) followed by (ii) efficient gettering at lower temperature should be used to handle precipitated metal impurities. This second gettering step can be a second isothermal low-temperature annealing immediately following the high temperature step or a controlled ramping down of the temperature.

4. Dislocations

So far, we have discussed the effect of dislocations mainly in terms of their role as nucleation sites for metal silicide precipitates. In addition, point defects including TM impurities may segregate in the dislocation strain field [25] or bind to the dislocation core. Both processes are of considerable importance since the combined action of deep states due to metal impurities and shallow bands related to the strain-field of dislocations may drastically enhance the recombination activity of dislocations [26]. The driving force for segregation in the dislocation strain field is mainly the strain energy contribution to the chemical potential of an impurity atom with a different size as the matrix. The related 'binding energies' are below 1 eV [25]. 'Chemical' binding of metal impurities to the core of different types of dislocations has recently been studied theoretically for the case of substitutional copper. Binding energies on the order of 2 eV are obtained [27] indicating that a considerable fraction of impurities may be bound to dislocation cores even at high temperatures which would strongly affect gettering kinetics. Fig. 5(a) shows the line concentration of gold bound to dislocations for a total gold concentration of 10^{14} cm^{-3} and a dislocation density of 10^8 cm^{-2} as a function the binding energy E_b. For a temperature of $T = 800\,^{\circ}$C about 50% of the gold atoms is bound to dislocations for $E_b \simeq 1.5$ eV and virtually all gold is gathered at dislocations for $E_b \simeq 2.0$ eV. This situation is a realistic estimate since experimental

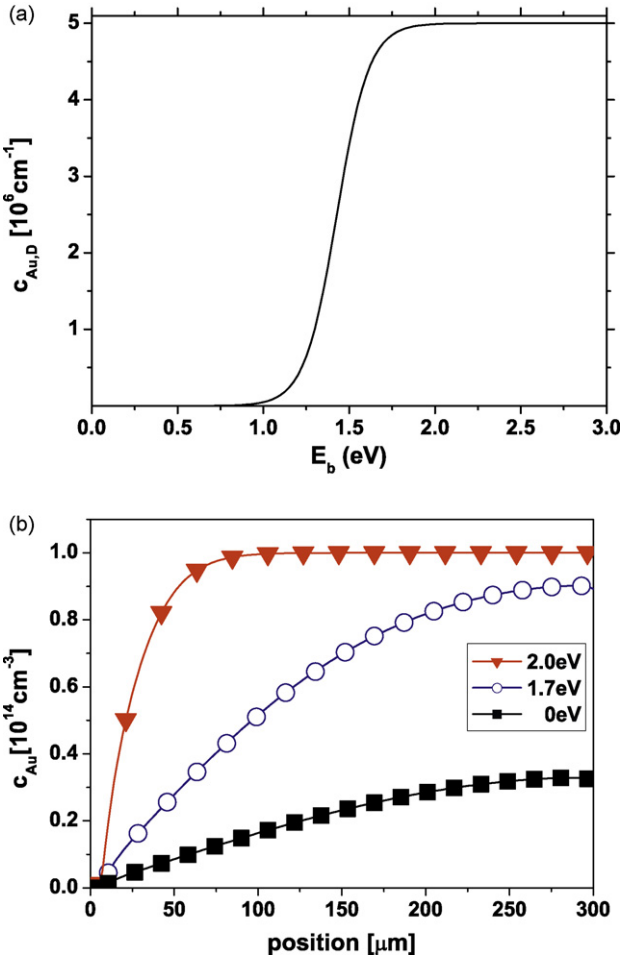

Fig. 5. Binding of gold to dislocations (dislocaton density: 10^8 cm^{-2}, total gold concentration $c_{Au,T} = 5 \times 10^{14}$ cm^{-3}): (a) line concentration $c_{Au,D}$ of gold bound to the dislocation core as a function of binding energy, E_b, at $T = 800^\circ$ C and (b) PDG of gold at 800 ° C in silicon with a dislocation density of 10^8 cm^{-2} for binding energies of $E_b = 0$ eV (squares), $E_b = 1.7$ eV (open circles), and $E_b = 2.0$ eV (triangles).

diffusion data point to binding energies of even 2.7 eV [28]. Such strong binding would dramatically slow down PDG kinetics as can be deduced from the simulations shown in Fig. 5(b): for PDG of gold at 800 ° C no interaction of gold and dislocations yields a strong gettering effect, whereas simulations show a strongly reduced gettering efficiency for $E_b = 1.7$ eV and virtually no reduction of the gold concentration for $E_b = 2.0$ eV.

5. Summary and conclusion

In this work we have discussed the effects of dislocations interacting with transition metal impurities on the kinetics of phosphorus diffusion gettering. Starting out from heterogeneous precipitation of fast diffusing metal impurities the competition between different types of nucleation sites has been considered and its effect on the spatial distribution of metal silicide precipitates after high temperature processing or crystal growth has been demonstrated. Once metal impurities are precipitated as metal silicides PDG kinetics can be classified as precipitate dissolution-limited for $T_G < T_{eq}$ and phosphorus-diffusion-limited for $T_G > T_{eq}$, where T_G and T_{eq} denote the gettering temperature and the temperature where the metal impurity concentration is equal to its solubility, respectively. Gettering simulations show that in the first regime gettering proceeds under persistent precipitate dissolution which is the rate-limiting process. In the second regime, precipitate have precipitated at the onset of gettering and kinetics are limited by the formation of the gettering layer, i.e the highly P-doped silicon region.

In this respect, aluminum gettering (AlG) should be superior to PDG since the formation of the Al:Si liquid serving as the gettering layer is very fast. In fact, experimental results for AlG of cobalt in silicon show that for $T_G > T_{eq}$ kinetics are just limited by diffusion of interstitially dissolved cobalt [29,19]. Technologically, however, the potential of AlG is not exploited during solar cell processing since typical conditions for back contact firing and backsurface field formation are not optimised in terms of gettering.

Finally, binding of impurity atoms to dislocation cores has been discussed in terms of binding energies and their effect on gettering kinetics. For values of $E_b = 2$ eV strong binding should occur even at elevated temperature which would considerably slow down PDG kinetics. Further theoretical and experimental work is needed to describe this process more quantitatively and verify its significance for multicrystalline silicon materials for photovoltaic applications.

Acknowledgements

This work was financially supported by the Volkswagen foundation (SOBSI project). We gratefully acknowledge T. Wilhelm and M. Reiche for providing hydrophobically bonded wafers. One of us (D.A.) gratefully acknowledges a scholarship from the Egyptian government.

References

[1] A.A. Istratov, T. Buonassisi, R.J. McDonald, A.R. Smith, R. Schindler, J.A. Rand, J.P. Kalejs, E.R. Weber, J. Appl. Phys. 94 (2003) 6552.
[2] T. Buonassisi, A.A. Istratov, M.D. Pickett, M. Heuer, J.P. Kalejs, G. Hahn, M.A. Marcus, B. Lai, Z. Cai, S.M. Heald, T.F. Ciszek, R.F. Clark, D.W. Cunningham, A.M. Gabor, R. Jonczyk, S. Narayanan, E. Sauar, E.R. Weber, Prog. Photovolt: Res. Appl. 14 (2006) 513.
[3] T. Buonassisi, M. Heuer, A.A. Istratov, M.D. Pickett, M.A. Marcus, B. Lai, Z. Cai, S.M. Heald, E.R. Weber, Acta Mater. 55 (2007) 6119.
[4] C. Rudolf, P. Saring, L. Stolze, M. Seibt, this volume.
[5] P. Saring, C. Rudolf, L. Stolze, M. Seibt, this volume.
[6] G. Kissinger, J. Dabrowsiki, A. Sattler, C. Seuring, T. Müller, H. Richter, W. von Ammon, J. Electrochem. Soc. 154 (2007) H454.
[7] M. Seibt, Mater. Res. Soc. Symp. Proc. 262 (1992) 957.
[8] M. Seibt, V. Kveder, W. Schröter, O. Voß, Phys. Stat. Sol. (A) 202 (2005) 911.
[9] M. Seibt, R. Khalil, V. Kveder, W. Schröter, Appl. Phys. A, in press, doi:10.1007/s00339-008-5027-8.
[10] A. Broniatowski, C. Haut, Phil. Mag. Lett. 62 (1994) 407.
[11] R. Rizk, X. Portier, G. Allais, G. Nouet, J. Appl. Phys. 76 (1994) 952.
[12] A. Ourmazd, W. Schröter, Appl. Phys. Lett. 45 (1984) 781.
[13] D. Gilles, E.R. Weber, S.K. Hahn, Phys. Rev. Lett. 64 (1990) 196.
[14] K. Graff, Metal Impurities in Silicon-Device Fabrication, Springer, Berlin, 1995.
[15] M. Seibt, K. Graff, J. Appl. Phys. 63 (1989) 4444.
[16] K. Honda, A. Ohsawa, N. Toyokura, Appl. Phys. Lett. 46 (1985) 582.
[17] H. Wendt, H. Cerva, V. Lehmann, W. Palmer, J. Appl. Phys. 65 (1989) 2402.
[18] M. Reiche, Phys. Stat. Sol. (A) 203 (2006) 747–759.
[19] M. Seibt, A. Sattler, C. Rudolf, O. Voß, V. Kveder, W. Schröter, Phys. Stat. Sol. (A) 203 (2006) 696.
[20] V. Kveder, W. Schröter, A. Sattler, M. Seibt, Mater. Sci. Eng. B 71 (2000) 175.
[21] E. Spiecker, M. Seibt, W. Schröter, Phys. Rev. B 55 (1997) 9577.
[22] E.Ö. Sveinbjörnsson, O. Engström, U. Södervall, J. Appl. Phys. 73 (1993) 7311.
[23] R. Kühnapfel, W. Schröter, Mater. Sci. Forum 10–12 (1986) 151.
[24] W. Schröter, V. Kveder, M. Seibt, A. Sattler, E. Spiecker, Solar Energy Mater. Solar Cells 72 (2002) 299.
[25] R. Bullough, R.C. Newman, Prog. Semicond. 7 (1963) 100.
[26] V. Kveder, M. Kittler, W. Schröter, Phys. Rev. B 63 (2001) 115206.
[27] N. Fujita, R. Jones, S. Öberg, P.R. Briddon, A.T. Blumenau, Solid State Phenom. 131–133 (2008) 259.
[28] A. Rodriguez, H. Bracht, I. Yonenaga, J. Appl. Phys. 95 (2004) 7841.
[29] A. Sattler, Ph.D. Thesis, Göttingen 2003, Cuvillier, Göttingen, 2002. ISBN: 3-89873-856-6.